Journal of Sound and Vibration (2002) **251**(5), 875–890
doi:10.1006/jsvi.2001.4018, available online at http://www.idealibrary.com on IDEAL®

QUASI-PERIODIC VIBRATION OF CRACKED ROTOR ON FLEXIBLE BEARINGS

Y. P. Pu, J. Chen, J. Zou and P. Zhong

The State Key Lab of the Vibration, Shock & noise, Shanghai Jiao Tong University, Shanghai 200030, *People's Republic of China. E-mails: Michaelpu@sina.com, Jinchen@mail.sjtu.edu.ch*

(*Received* 16 *January* 2001, *and in final form* 28 *September* 2001)

A cracked rotor on flexible bearings is studied in this paper. The vibration of such a system has many complexities because of the crack and bearing flexibility. However, if the properties of the bearings are known, the system can be simplified by supposing that, the vibration due to weight is dominant. Equations of motion are derived, and a linear system in which the crack has been considered as an external disturbance described by a series of trigonometric functions is obtained. Consequently, the quasi-periodic vibrations of the rotor and bearings are established by harmonic balance method and approximate values of the vibration determined by truncating the higher order terms. It is believed that the simulated results will be useful for crack detection in the case of weight-dominant rotors.

1. INTRODUCTION

There has been extensive research on the vibration behaviour of cracked rotors and the use of response characteristics to detect cracks. An excellent review of the field of the dynamics of cracked rotors and of different detection procedures to diagnose fracture damage has been carried out by Wauer [1]. The state-of-the-art has been presented by Dimarogonas and Papadopoulos in references [2, 3]. Sekhar [4, 5] and Qian [6] studied a cracked shaft by FEM. Ratan and Baruh [7, 8] proposed some new methods to detect and locate a crack in a rotor, but only considered a constantly opened crack. Wauer [9] and Rajab [10] also studied the distributed parameter rotor by using a rotating Timoshenko shaft and derived the governing equations of motion of the rotor. Similar work has been done by Rizos and Tsai [11, 12]. Collins [13], Armon [14] and Söffker [15] contributed their investigations on crack detection in different respects. Seibold [16] used EKF method; a time domain method, to study the localization of cracks. There has been flourishing research in this domain. The above list is merely a small part. However, most of the previous work involved the rotor supported on ideal bearings. As we know, bearing forces can affect the vibration of the shaft. Coupled bearing forces and vibration of the shaft lead to many complexities in a rotor system. It is possible to simplify the problem if the vibrations remain small in comparison to the sag of the rotor under its weight (weight-dominant rotor), since the non-linear equations of motion can be transformed into linear, periodically time-variant equations [17, 18]. However, even with weight dominance in the displacement, a generally valid description in the sense of similarity theory is only possible in a few diagrams if the crack model is restricted to "strong" parameters. Only then, are the results independent of the specific geometrical dimensions of the shaft. Comparison of three different models of

0022-460X/02/$35.00

a cracked hollow shaft in reference [19] shows that, when the crack depth is not more than half of the shaft radius, a simple hinge model is a good representation of the cyclic stiffness variation and for stability limits. The same is true for a solid shaft.

The aim of this paper is to obtain a stable response of a rotor–bearing system when the condition of the "weight dominance" is available. The "breathing" of the crack has been simulated by "hinge mechanism", and the flexible single-degree-of-freedom (S.D.O.F.) rotor supported on flexible bearings is proposed. The crack is transformed into an external disturbance, described by a series of trigonometric functions. Consequently, the bearing forces and interactions between a lumped-mass disc and flexible shaft have been represented by a series of trigonometric functions [20]. The vibrations of the lumped-mass disc, bearing forces and the interactions between the disc and the shaft were obtained by using harmonic balance method.

2. CRACK MODEL

The equation of motion for a simple rotor with a cracked shaft has the following form:

$$M\ddot{u} + D\dot{u} + S(u, t)u = p_0 + p_w, \tag{1}$$

where M is the mass matrix, D is the damping matrix, p_0 is the weight, and p_w is the periodic excitation.

The stiffness matrix $S(u, t)$, which in the general case is non-linear and time-variant, can be split into

$$S(u, t) = S_0 + \Delta S(u, t), \tag{2}$$

where S_0 is the diagonal stiffness matrix of the uncracked shaft. $\Delta S(u, t)$ is the additive (negative) crack matrix, which is dependent both on the displacements u and on the rotation angle of the rotor. However, a crack in a rotor usually causes a small change in its stiffness.

The vibrational response of the rotor can also be split into

$$u(t) = u_0 + \Delta u(t), \tag{3}$$

where, u_0 is the static deflection of the uncracked shaft, and $\Delta u(t)$ is the vector describing the vibrational behaviour.

If weight dominance is assumed for the elastic deflection, considering $\Delta S(u, t) \to \Delta S(t)$, then the non-linear equation of motion (1) can be modified by substitution from equations (2), (3) to yield

$$M\Delta\ddot{u} + D\Delta\dot{u} + [S_0 + \Delta S(t)]\Delta u = -\Delta S(t)u_0 + p_w. \tag{4}$$

This equation is now linear, but periodically time-variant. If the stability of the rotor is guaranteed; $\Delta S(t) \times \Delta u(t) \approx 0$, the forced vibrations can be determined from the following time-invariant system:

$$M\Delta\ddot{u} + D\Delta\dot{u} + S_0\Delta u = -\Delta S(t)u_0 + p_w. \tag{5}$$

Apparently, in equation (5), the effect of the crack has been transformed into an external excitation of the vibrational system. The above-mentioned processing is described in detail in a paper by the Gasch [3].

Under the assumption of "hinge" model, the breathing of the crack is described by a rectangular function, which can be written as

$$f(t) = \begin{cases} 1 & \cos\omega t > 0, \\ 0 & \cos\omega t < 0. \end{cases} \tag{6}$$

The steering function, $f(t)$ for the hinge switches from 1 (open) to 0 (closed), can also be expressed by a Fourier series [20]:

$$f(t) = 1/2 + 2/\pi\cos\omega t - 2/(3\pi)\cos 3\omega t + 2/(5\pi)\cos 5\omega t - 2/(7\pi)\cos 7\omega t \cdots. \tag{7}$$

Provided that the change in stiffness due to an open crack is Δk, and that the crack "breathes" according to "hinge mechanism", the additional disturbing forces in the stationary co-ordinates in y and x directions, respectively, can be expressed as

$$f_x = 1/2 \times \Delta k \times u_{y0} \times f(t) \times \sin 2\omega t, \tag{8a}$$

$$f_y = 1/2 \times \Delta k \times u_{y0} \times f(t) \times (1 + \cos 2\omega t). \tag{8b}$$

Considering equation (6):

$$f_x = \frac{1}{2}\Delta k u_{y0}\left\{\frac{5}{6\pi}\sin\omega t + \frac{1}{2}\sin 2\omega t + \frac{3}{10\pi}\sin 3\omega t - \frac{4}{21\pi}\sin 5\omega t - \frac{1}{5\pi}\sin 7\omega t \cdots\right\}, \tag{9a}$$

$$f_y = \frac{1}{2}\Delta k u_{y0}\left\{\frac{1}{2} + \frac{7}{6\pi}\cos\omega t + \frac{1}{2}\cos 2\omega t + \frac{1}{30\pi}\cos 3\omega t - \frac{6}{105\pi}\cos 5\omega t - \frac{12}{35\pi}\cos 7\omega t \cdots\right\}. \tag{9b}$$

Similarly, the change of the inertia moment due to the open crack can also be transformed into external moment. The steering function $f(t)$ is also available:

$$m_{yz} = 1/2 \times \Delta I \times \theta_0 \times f(t) \times (1 + \cos 2\omega t), \tag{10a}$$

$$m_{xz} = 1/2 \times \Delta I \times \theta_0 \times f(t) \times \sin 2\omega t, \tag{10b}$$

where ΔI is the change of the angular stiffness due to the open crack, θ_0 is the static inclination of the disc, m_{yz} and m_{xz} are the moments in y–z plane and moments in x–z plane respectively. Then, the additional disturbing moments can be written as

$$m_{xz} = 1/2\,\Delta I\theta_0\left\{\frac{5}{6\pi}\sin\omega t + \frac{1}{2}\sin 2\omega t + \frac{3}{10\pi}\sin 3\omega t - \frac{4}{21\pi}\sin 5\omega t - \frac{1}{5\pi}\sin 7\omega t \cdots\right\}, \tag{11a}$$

$$m_{yz} = 1/2\,\Delta I\theta_0\left\{\frac{1}{2} + \frac{7}{6\pi}\cos\omega t + \frac{1}{2}\cos 2\omega t + \frac{1}{30\pi}\cos 3\omega t - \frac{6}{105\pi}\cos 5\omega t - \frac{12}{35\pi}\cos 7\omega t \cdots\right\}. \tag{11b}$$

Considering equation (9), the additional forces can be written as

$$f_y = \sum_{i=1}^{n} Q_i \sin i\omega t, \qquad f_x = \sum_{i=1}^{n} P_i \cos i\omega t. \tag{12a,b}$$

Similarly, according to equation (11), the additional moments may be written as:

$$m_{yz} = \sum_{i=1}^{n} W_i \sin i\omega t, \qquad m_{xz} = \sum_{i=1}^{n} O_i \cos i\omega t. \tag{13a,b}$$

3. ROTOR AND BEARING SYSTEM

The total deflection of the rotor is the vector sum of the deflection of the rotor relative to the shaft ends plus that of the shaft ends in the bearings (Figure 1). The deflection of the shaft ends in the bearing is related to the force transmitted through the bearings by the bearing stiffness and damping coefficients as follows:

$$ {}_a f_x = k_{xx} \times {}_a m + k_{xy} \times {}_a n + c_{xx} \times {}_a \dot{m} + c_{xy} \times {}_a \dot{n}, \tag{14a} $$

$$ {}_a f_y = k_{yx} \times {}_a m + k_{yy} \times {}_a n + c_{yx} \times {}_a m + c_{yy} \times {}_a n, \tag{14b} $$

where ${}_a m$ and ${}_a n$ are the instantaneous displacements of the shaft ends relative to the bearings in the horizontal and vertical directions, respectively, and take the form

$$ {}_a m = \sum_{i=1}^{n} {}_a M_{1i} \sin(i\omega t) + \sum_{i=1}^{n} {}_a M_{2i} \cos(i\omega t), \tag{15a} $$

$$ {}_a n = \sum_{i=1}^{n} {}_a N_{1i} \cos(i\omega t) + \sum_{i=1}^{n} {}_a N_{2i} \sin(i\omega t), \tag{15b} $$

$$ {}_a f_x = \sum_{i=1}^{n} {}_a F_{x1i} \sin(i\omega t) + \sum_{i=1}^{n} {}_a F_{x2i} \cos(i\omega t), \tag{15c} $$

$$ {}_a f_y = \sum_{i=1}^{n} {}_a F_{y1i} \cos(i\omega t) + \sum_{i=1}^{n} {}_a F_{y2i} \sin(i\omega t). \tag{15d} $$

Comparing coefficients of $\sin(i\omega t)$ and $\cos(i\omega t)$ on each side of both equations results in the matrix equation:

$$ \begin{Bmatrix} {}_aF_{x11} \\ \vdots \\ {}_aF_{x1n} \\ {}_aF_{x21} \\ \vdots \\ {}_aF_{x2n} \\ {}_aF_{y11} \\ \vdots \\ {}_aF_{y1n} \\ {}_aF_{y21} \\ \vdots \\ {}_aF_{y2n} \end{Bmatrix} = \begin{bmatrix} k_{xx} & \cdots & 0 & -\omega c_{xx} & \cdots & 0 & -\omega c_{xy} & \cdots & 0 & k_{xy} & \cdots & 0 \\ \vdots & \ddots & \vdots & \vdots & \ddots & \vdots & \vdots & \ddots & \vdots & \vdots & \ddots & \vdots \\ 0 & \cdots & k_{xx} & 0 & \cdots & -n\omega c_{xx} & 0 & \cdots & -n\omega c_{xy} & 0 & \cdots & k_{xy} \\ \omega c_{xx} & \cdots & 0 & k_{xx} & \cdots & 0 & k_{xy} & \cdots & 0 & \omega c_{xy} & \cdots & 0 \\ \vdots & \ddots & \vdots & \vdots & \ddots & \vdots & \vdots & \ddots & \vdots & \vdots & \ddots & \vdots \\ 0 & \cdots & n\omega c_{xx} & 0 & \cdots & k_{xx} & 0 & \cdots & k_{xy} & 0 & \cdots & n\omega c_{xy} \\ \omega c_{yx} & \cdots & 0 & k_{yx} & \cdots & 0 & k_{yy} & \cdots & 0 & \omega c_{yy} & \cdots & 0 \\ \vdots & \ddots & \vdots & \vdots & \ddots & \vdots & \vdots & \ddots & \vdots & \vdots & \ddots & \vdots \\ 0 & \cdots & n\omega c_{yx} & 0 & \cdots & k_{yx} & 0 & \cdots & k_{yy} & 0 & \cdots & n\omega c_{yy} \\ k_{yx} & \cdots & 0 & -\omega c_{yx} & \cdots & 0 & -\omega c_{yy} & \cdots & 0 & k_{yy} & \cdots & 0 \\ \vdots & \ddots & \vdots & \vdots & \ddots & \vdots & \vdots & \ddots & \vdots & \vdots & \ddots & \vdots \\ 0 & \cdots & k_{yx} & 0 & \cdots & -n\omega c_{yx} & 0 & \cdots & -n\omega c_{yy} & 0 & \cdots & k_{yy} \end{bmatrix} \begin{Bmatrix} {}_aM_{11} \\ \vdots \\ {}_aM_{1n} \\ {}_aM_{21} \\ \vdots \\ {}_aM_{2n} \\ {}_aN_{11} \\ \vdots \\ {}_aN_{1n} \\ {}_aN_{21} \\ \vdots \\ {}_aN_{2n} \end{Bmatrix} $$

which can be expressed more simply as

$$ \{{}_a F_b\} = [{}_a I]\{{}_a v\}. \tag{16} $$

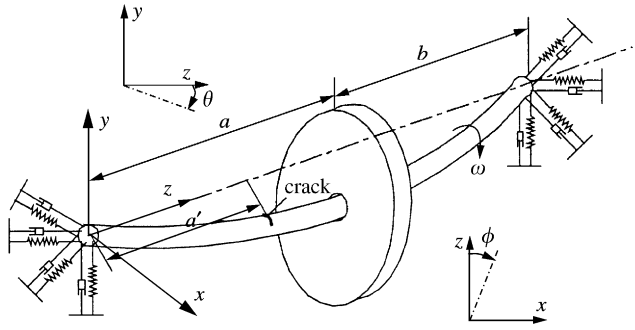

Figure 1. Single mass rotor on a light shaft, running in fluid lubricated bearing.

Similarly, another equation describing the forces transmitted through the bearing at the other end of the machine may be written as

$$\{{}_bF_b\} = [{}_bI]\{{}_bv\}. \tag{17}$$

Combining equations (16) and (17):

$$\begin{Bmatrix} {}_aF_b \\ {}_bF_b \end{Bmatrix} = \begin{bmatrix} {}_aI & 0 \\ 0 & {}_bI \end{bmatrix} \begin{Bmatrix} {}_av \\ {}_bv \end{Bmatrix} \tag{18}$$

which can be abbreviated as

$$\{F_b\} = [I]\{v\}. \tag{19}$$

The magnitude of the reaction forces transmitted by the bearings can also be evaluated in terms of the forces applied to the shaft by the rotor. Considering the shaft to behave as a simply supported beam carrying a point force and moment at the location of the rotor shown in Figure 2, the vertical reaction forces at the shaft ends are

$${}_af_y = (1 - a/l)F_y + (1/l)M_{yz}, \tag{20a}$$

$${}_bf_y = (a/l)F_y - (1/l)M_{yz} \tag{20b}$$

and similarly, the forces in the horizontal direction may be written as

$${}_af_x = (1 - a/l)F_x + (1/l)M_{xz}, \tag{20c}$$

$${}_bf_x = (a/l)F_x - (1/l)M_{xz}. \tag{20d}$$

Recognizing that the forces and moments applied to the shaft by the rotor vary sinusoidally, we arrive at

$$F_y = \sum_{i=1}^{n} F_{y1i}\cos(i\omega t) + \sum_{i=1}^{n} F_{y2i}\sin(i\omega t), \tag{21a}$$

$$F_x = \sum_{i=1}^{n} F_{x1i}\sin(i\omega t) + \sum_{i=1}^{n} F_{x2i}\cos(i\omega t), \tag{21b}$$

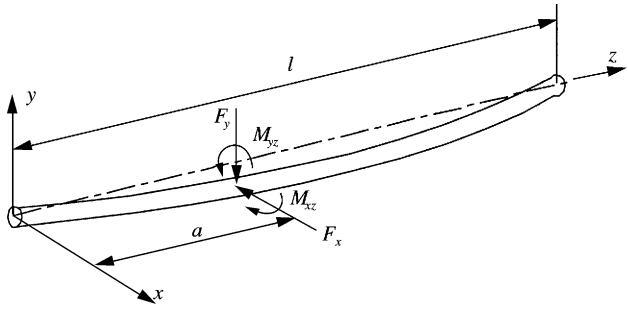

Figure 2. Simply supported shaft carrying a point force and moment at the location of the rotor.

$$M_{yz} = \sum_{i=1}^{n} M_{yz1i}\cos(i\omega t) + \sum_{i=1}^{n} M_{yz2i}\sin(i\omega t), \tag{21c}$$

$$M_{xz} = \sum_{i=1}^{n} M_{xz1i}\sin(i\omega t) + \sum_{i=1}^{n} M_{xz2i}\cos(i\omega t). \tag{21d}$$

Substituting these expressions into equation (8), and comparing coefficients of $\sin(i\omega t)$ and $\cos(i\omega t)$ leads to the matrix equation

$$\{F_b\} = [A]\{F_s\} + [A_c]\{F_{crack}\}, \tag{22}$$

where $[A]$ and $[A_c]$ are determined by the geometrical parameters of the rotor and

$$\{F_s\} = \Big[F_{y11}, \ldots, F_{y1n}, \overbrace{M_{yz11}, \ldots, M_{yz1n}}^{n}, F_{x11}, \ldots, F_{x1n}, M_{xz11}, \ldots, M_{xz1n}, F_{y21}, \ldots,$$

$$F_{y2n}, \ldots, \ldots, M_{xz21}, \ldots, M_{xz2n} \Big]^{\mathrm{T}},$$

$$[F_b\} = \Big[{}_aF_{x11}, \ldots, {}_aF_{x1n}, \overbrace{{}_aF_{x21}, \ldots, {}_aF_{x2n}}^{n}, {}_aF_{y11}, \ldots, F_{y1n}, {}_aF_{y21}, \ldots, {}_aF_{y2n}, {}_bF_{x11}, \ldots,$$

$${}_bF_{x1n}, \ldots, \ldots, {}_bF_{y21}, \ldots, {}_bF_{y2n} \Big]^{\mathrm{T}}.$$

The subscripts b and s indicate loads applied to the bearing and rotor respectively. It is now possible to obtain expressions for the deflection at the bearings in terms of the forces and moments applied to the shaft. This can be done by substituting equation (22) into equation (19):

$$\{v\} = [I]^{-1}([A]\{F_s\} + [A_c]\{F_{crack}\}). \tag{23}$$

Recognizing that these shaft displacements vary sinusoidally such that x_r, y_r, ϕ, and θ may be written in the form

$$x_r = \sum_{i=1}^{n} X_{1i}\sin(i\omega t) + \sum_{i=1}^{n} X_{2i}\cos(i\omega t), \tag{24a}$$

$$y_r = \sum_{i=1}^{n} Y_{1i}\cos(i\omega t) + \sum_{i=1}^{n} Y_{2i}\sin(i\omega t), \tag{24b}$$

$$\phi = \sum_{i=1}^{n} \Phi_{1i}\sin(i\omega t) + \sum_{i=1}^{n} \Phi_{2i}\cos(i\omega t), \tag{24c}$$

$$\theta = \sum_{i=1}^{n} \Theta_{1i}\cos(i\omega t) + \sum_{i=1}^{n} \Theta_{2i}\sin(i\omega t) \tag{24d}$$

and considering the shaft to be rigid for the moment, the horizontal deflection of the shaft at the rotor must be

$$x_r = {}_am + ({}_am - {}_bm)\times(d/l) = (1 - d/l){}_am + (d/l){}_bm \tag{25a}$$

and the slope of the shaft in the x–z plane will be

$$\phi = ({}_am - {}_bm)/l. \tag{25b}$$

Similarly, for motion in the vertical direction and y–z plane:

$$y_r = {}_an + ({}_an - {}_bn)\times(d/l) = (1 - d/l){}_an + (d/l){}_bn, \tag{25c}$$

$$\theta = ({}_an - {}_bn)/l. \tag{25d}$$

Substituting x_r, ϕ, y_r and θ from equation (24), together with expressions for ${}_am$, ${}_an$, ${}_bm$ and ${}_bn$ from equation (15a), (15b) into equation (25), and comparing coefficients of $\sin(i\omega t)$ and $\cos(i\omega t)$ on either side of the resulting four equations, the following matrix equation is obtained:

$$\{u_b\} = [B]\{v\}. \tag{26}$$

Substituting for $\{v\}$ from equation (23):

$$\{u_b] = [B][I]^{-1}([A]\{F_s\} + [A_c]\{F_{crack}\}), \tag{27}$$

where the matrix $[B]$ is also determined by geometrical parameters of the rotor and:

$$\{u_b\} = [Y_{11}, \ldots, Y_{1n}, \Theta_{11}, \ldots, \Theta_{1n}, X_{11}, \ldots, X_{1n}, \Phi_{11}, \ldots, \Phi_{1n}, Y_{21}, \ldots,$$
$$Y_{2n}, \ldots, \ldots, \Phi_{21}, \ldots, \Phi_{2n}]^{\mathrm{T}}.$$

In order to obtain the net rotor deflection under a given load, we must add the deflection due to deformation of the shaft to that which has been calculated in equation (27). As we know, the crack can be considered as an external disturbing force when the maximum amplitude of the vibration is far less than the stationary deflection of the rotor. Therefore, the deflection at the disk due to deformation of the shaft:

$$\{u_s\} = [\alpha]\{F_s\} + [\alpha_c]\{F_{crack}\}, \tag{28}$$

where $\{F_{crack}\}$ is the disturbing force due to the crack, $[\alpha]$ and $[\alpha_c]$ are the flexibility matrixes when loaded by $\{F_s\}$ and by $\{F_{crack}\}$ respectively. Consequently, the net rotor deflection is

$$\{u\} = \{u_b\} + \{u_s\} = ([B][I]^{-1}[A] + [\alpha])\{F_s\} + ([B][I]^{-1}[A_c] + [\alpha_c])\{F_{crack}\}$$
$$= [D]\{F_s\} + [D_c]\{F_{crack}\}. \tag{29}$$

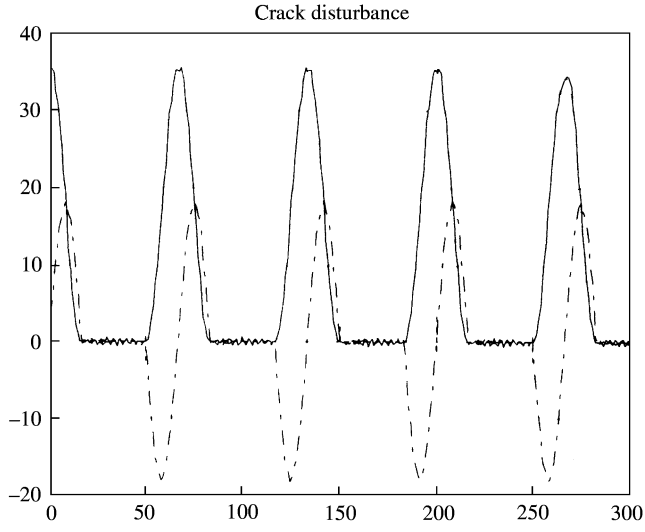

Figure 3. The crack disturbance ($h_c/h = 0{\cdot}1$): ——, y direction; — – —, x direction.

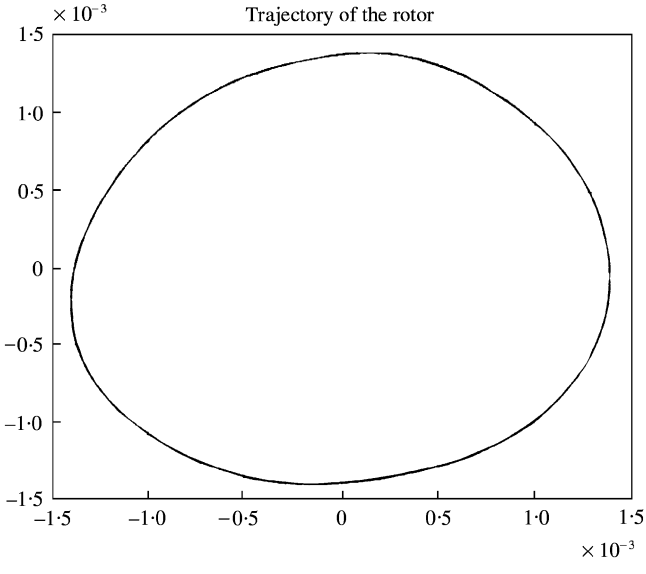

Figure 4. Trajectory of the rotor: $h_c/h = 0{\cdot}1$, $\beta = 0$, $e = 0{\cdot}5$ mm.

The equation of motion for the rotor, allowing for motion in the x, y, θ and ϕ senses, can be written as

$$me\omega^2 \sin \omega t - F_y = m\ddot{y}_r, \tag{30a}$$

$$- M_{yz} = I_d \ddot{\theta}, \tag{30b}$$

$$me\omega^2 \cos \omega t - F_x = m\ddot{x}_r, \tag{30c}$$

$$- M_{xz} = I_d \ddot{\phi}. \tag{30d}$$

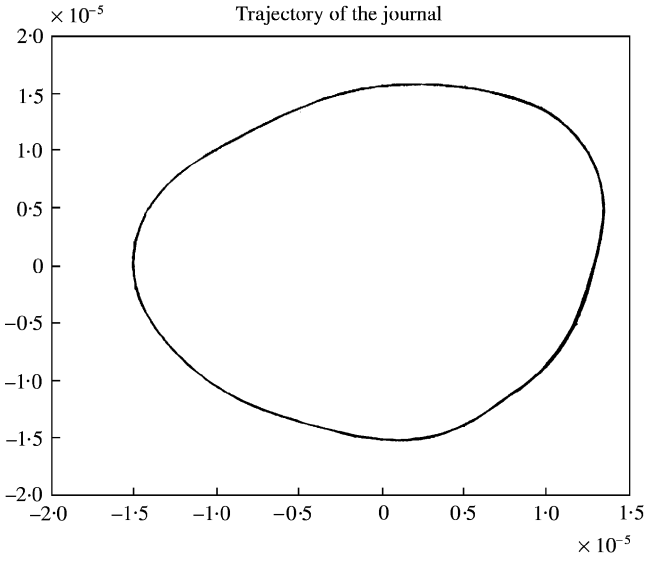

Figure 5. Trajectory of the journal: $h_c/h = 0{\cdot}1$, $\beta = 0$, $e = 0{\cdot}5$ mm.

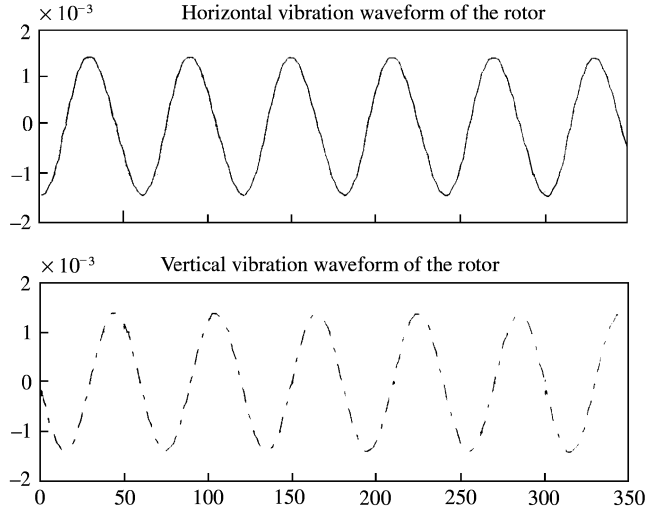

Figure 6. Amplitude–time waveform of the rotor vibration: $h_c/h = 0{\cdot}1$, $\beta = 0$, $e = 0{\cdot}5$ mm.

Substituting for F_y, F_x, M_{yz} and M_{xz} from equation (21) into equation (30), and abbreviating, we obtain the compact equation

$$\{f\} = \{F_s\} + [G]\{u\}, \tag{31}$$

where $[G]$ is composed of the mass and the moment of the rotor. Substituting for $\{F_s\}$ from equation (23) gives

$$\{f\} = [D]^{-1}(\{u\} - [D_c]\{F_{crack}\}) + [G]\{u\} \tag{32a}$$

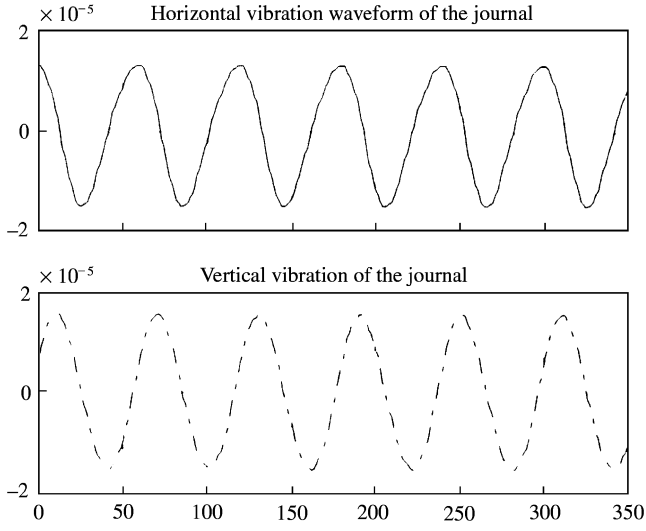

Figure 7. Amplitude–time waveform of the journal vibration: $h_c/h = 0{\cdot}1$, $\beta = 0$, $e = 0{\cdot}5$ mm.

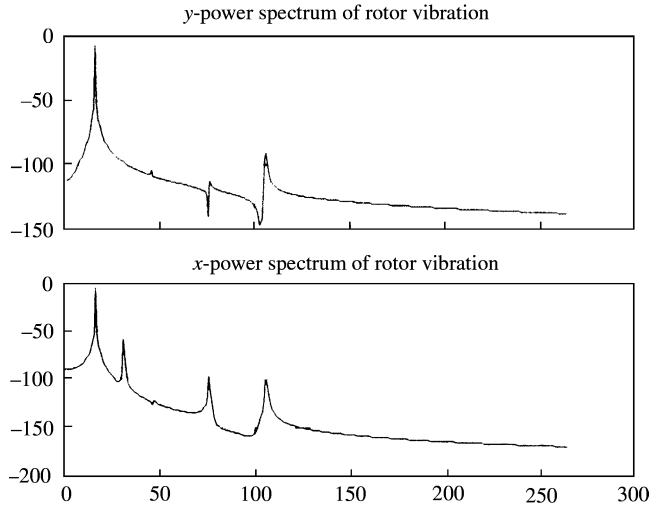

Figure 8. Noise-free power spectrum of rotor vibration: $h_c/h = 0{\cdot}1$, $\beta = 0$, $e = 0{\cdot}5$ mm.

or

$$\{f\} = ([D]^{-1} + [G])\{u\} - [D]^{-1}[D_c]\{F_{crack}\}. \tag{32b}$$

Equation (27) can be rearranged to give the response of the rotor as

$$\{u\} = [H]^{-1}(\{f\} + [L]\{F_{crack}\}). \tag{33}$$

The response of the rotor can be obtained from equation (33). The change of stiffness is expressed by an infinite series in equation (7). Considering equations (2), (7), (12), (19) and (22), it is apparent that this response is the series of the $\sin(i\omega t)$ and $\cos(i\omega t)$, namely, the

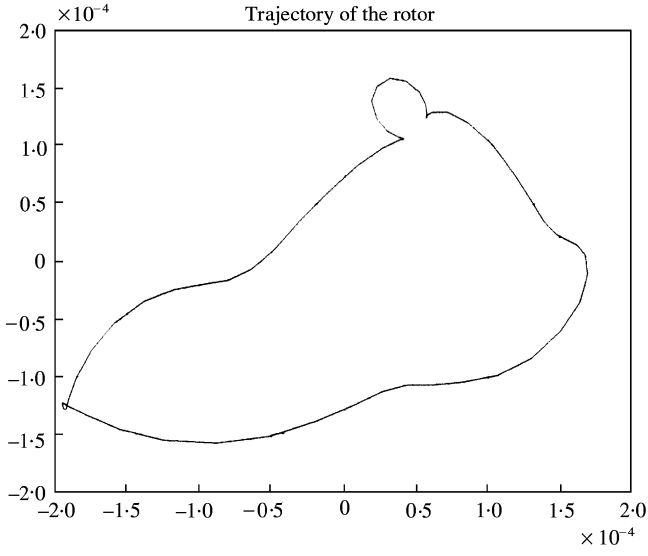

Figure 9. Trajectory of the rotor: $h_c/h = 0{\cdot}1$, $\beta = 0$, $e = 0{\cdot}05$ mm.

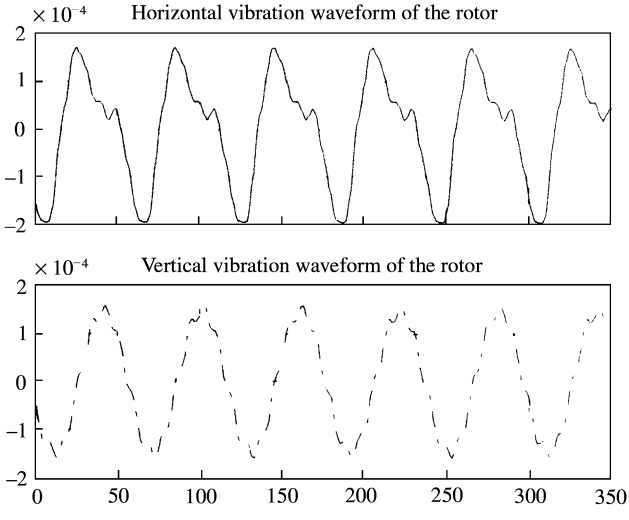

Figure 10. Amplitude–time waveform of the rotor vibration: $h_c/h = 0{\cdot}1$, $\beta = 0$, $e = 0{\cdot}05$ mm.

quasi-periodic vibration. Once the response of the rotor has been obtained, it is possible to calculate the vibration of the journals, and calculate the forces transmitted through the bearings and to find the load applied to shaft.

4. RESULTS AND DISCUSSION

In practice, it is impossible to calculate the response of the rotor when the function of the stiffness due to crack is considered as an infinite series, like equation (7). However, the main components of the response can be obtained by truncating the higher order terms in

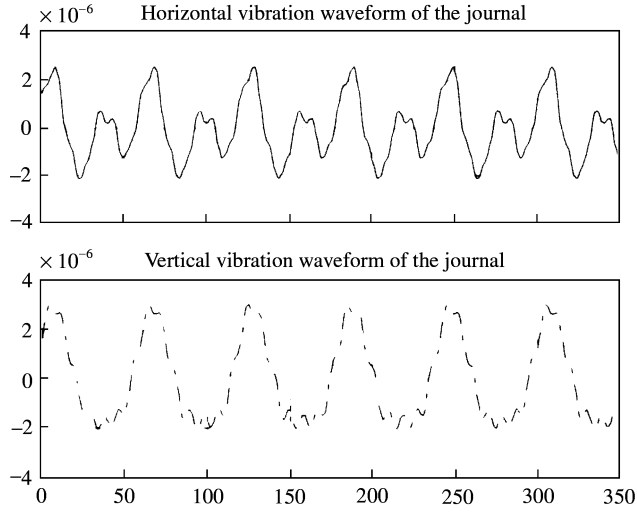

Figure 11. Amplitude–time waveform of the journal vibration: $h_c/h = 0{\cdot}1$, $\beta = 0$, $e = 0{\cdot}05$ mm.

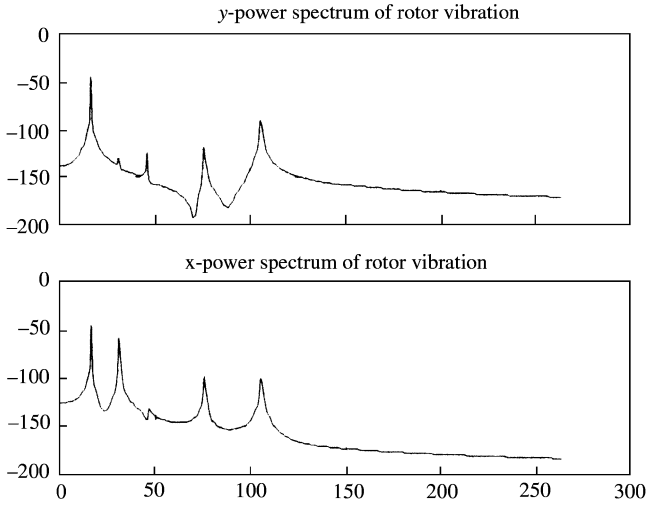

Figure 12. Noise-free power spectrum of rotor vibration: $h_c/h = 0{\cdot}1$, $\beta = 0$, $e = 0{\cdot}05$ mm.

TABLE 1

Geometric parameters of the rotor

Length of the shaft	The mass of the rotor	Diameter of the shaft
1·2 m	40 kg	0·03 m

equation (7). If only the first five terms are considered, in equations (9) and (11), the highest value of i in $\sin(i\omega t)$ and $\cos(i\omega t)$ will be 8, and no other excitation and disturbance (except the crack) can induce high order response. Hence, n in the previous equations is equal to 8. Subsequently, the response can be approximated.

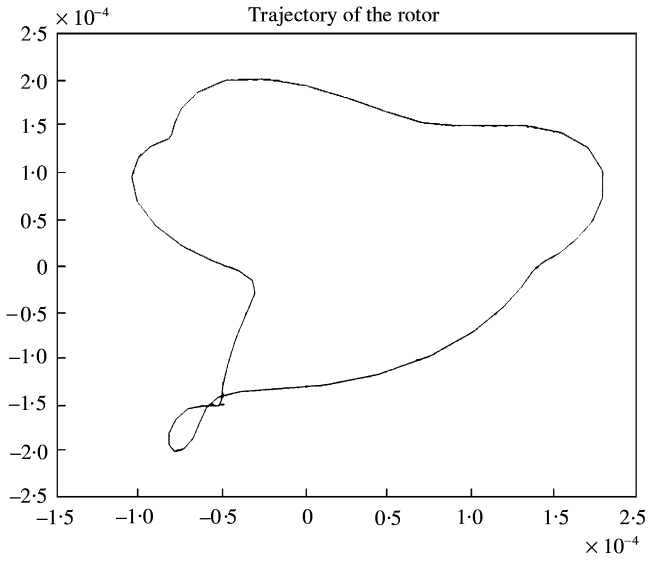

Figure 13. Trajectory of the rotor: $h_c/h = 0{\cdot}1$, $\beta = 60^\circ$, $e = 0{\cdot}05$ mm.

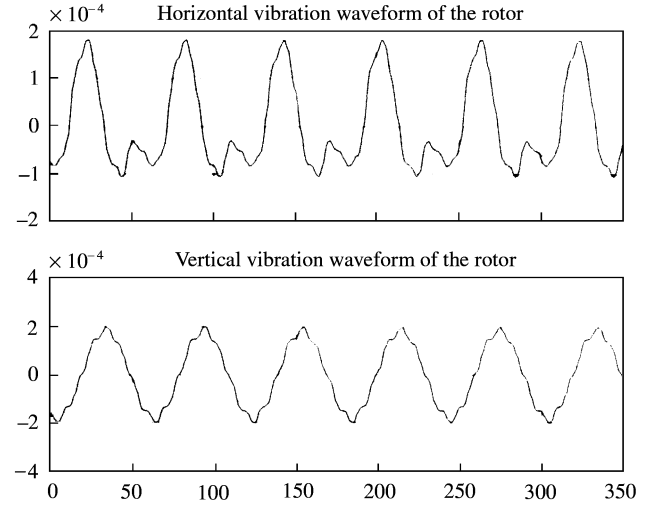

Figure 14. Amplitude–time waveform of the rotor vibration: $h_c/h = 0{\cdot}1$, $\beta = 60^\circ$, $e = 0{\cdot}05$ mm.

Simulating the rotor supported on a flexible bearing by a De Lavel rotor, the disc is located at the middle of the shaft, the geometrical parameters of the rotor are listed in Table 1.

Then the matrix describing how the load on the shaft is distributed to the bearings is found from equation (22). The relationship between the shaft displacement at the rotor and the shaft displacement at the bearings is given by equation (26). The shaft displacement at the rotor due to its flexibility is given by equation (28).

Provided that h_c is the local flexibility, h is the flexibility of the normal shaft, β is the angle between the directions of the crack and centrifugal force and $k_{xx} = k_{yy}$, $k_{xy} = k_{yx}$, $c_{xx} = c_{yy}$

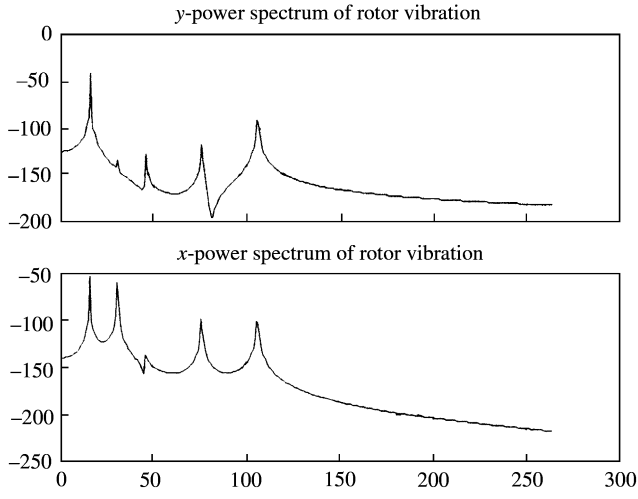

Figure 15. Noise-free power spectrum of rotor vibration: $h_c/h = 0{\cdot}1$, $\beta = 60^\circ$, $e = 0{\cdot}05$ mm.

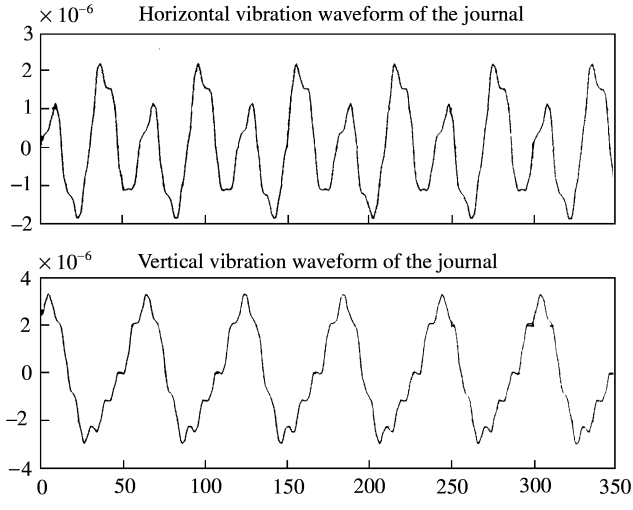

Figure 16. Amplitude–time waveform of the rotor vibration: $h_c/h = 0{\cdot}1$, $\beta = 60^\circ$, $e = 0{\cdot}05$ mm.

$c_{xy} = c_{yx}$, the trajectory and the vibration waveform of the centre of the rotor and of the journal can be calculated by using the method derived above. The results are shown in the following figures.

The crack disturbance is shown in Figure 3. The vertical disturbance is indicated by the solid line and the horizontal disturbance is indicated by the dashdotted line. The trajectories and the vibration waveform of the rotor and journal are shown in Figures 4–7, when the $h_c/h = 0{\cdot}1$, $\beta = 0$ and $e = 0{\cdot}5$ mm. The corresponding noise-free power spectrum of the rotor vibration is shown in Figure 8 from which one can find the quasi-periodic vibration of the rotor. When the eccentricity changes to $e = 0{\cdot}05$ mm, the results, correspondingly, are shown in Figures 9–12. It is obvious that the vibration due to unbalance is dominant when the centrifugal force is far larger than the crack disturbance. Both trajectories in Figures 4 and 5 are similar to a circle and the waveforms in Figures 6 and 7 are similar to sinusoid or

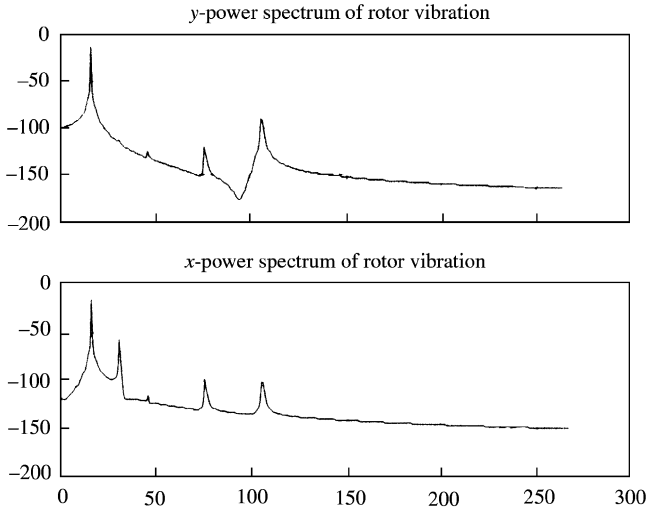

Figure 17. Noise-free power spectrum of rotor vibration: $h_c/h = 0{\cdot}1$, $\beta = 60^\circ$, $e = 0{\cdot}3$ mm.

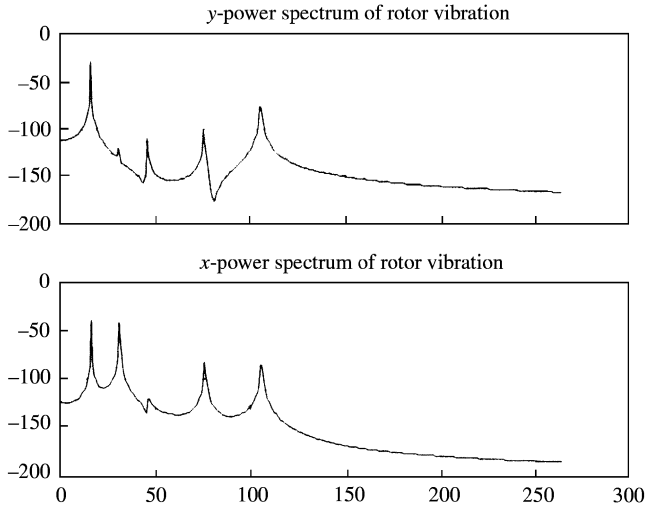

Figure 18. Noise-free power spectrum of rotor vibration: $h_c/h = 0{\cdot}3$, $\beta = 60^\circ$, $e = 0{\cdot}3$ mm.

cosine waveform. When the centrifugal force and the crack disturbance are comparative, the properties of the crack appear in the vibration signal. Like the result shown in Figures 9–12, comparing Figures 9, 10 and 11 to Figures 13, 14 and 16, the trajectory and the waveform are sensitive to the angle between the crack direction and centrifugal force changes, unlike for the power spectrum. To increase the crack disturbance, namely, increase the depth of the crack, obviously, the amplitude of the high order harmonic, such as second, third, fifth harmonic, will increase. Therefore, high order harmonic can be considered as a sign of a propagating crack, as shown in Figures 17 and 18.

Experimental validation of the simulated results will be reported by the author in the future paper that is underway.

ACKNOWLEDGMENTS

This work is supported by the National Fundamental Research Project of Science and Technology Development (People's Republic of China) (973, No.G1998020321).

REFERENCES

1. J. WAUER 1990 *Applied Mechanics Review* **43**, 13–17. On the dynamics of cracked rotors: a literature survey.
2. A. D. DIMAROGONAS and C. A. PAPADOPOULOS 1983 *Journal of Sound and Vibration* **91**, 583–593. Vibration of cracked shafts in bending.
3. C. A. PAPADOPOULOS and A. D. DIMAROGONAS 1987 *Journal of Sound and Vibration* **117**, 81–93. Coupled longitudinal and bending vibrations of a rotating shaft with an open crack.
4. A. S. SEKHAR and B. S. PRABHU 1992 *Journal of Sound and Vibration* **157**, 375–381. Crack detection and vibration characteristics of cracked shafts.
5. A. S. SEKHAR 1999 *Journal of Sound and Vibration* **223**, 497–512. Vibration characteristics of a cracked rotor with two open cracks.
6. G.-L. QIAN, S.-N. GU and J.-S. JIANG 1990 *Journal of Sound and Vibration* **138**, 233–243. The dynamic behaviour and crack detection of a beam with a crack.
7. S. RATAN, H. BARUH and J. RODRIGUEZ 1996 *Journal of Sound and Vibration* **194**, 67–82. On-line identification and location of rotor cracks.
8. H. BARUH and S. RATAN 1993 *Journal of Sound and Vibration* **166**, 21–30. Damage detection in flexible structures.
9. J. WAUER 1990 *International Journal of Solids and Structure* **26**, 901–914. Modelling and formulation of equations of motion for cracked rotating shafts.
10. M. D. RAJAB and A. AL-SABEEH 1991 *Journal of Sound and Vibration* **147**, 465–473. Vibration characteristics of cracked shafts.
11. P. F. RIZOS and N. ASPRAGATHOS 1990 *Journal of Sound and Vibration* **138**, 381–388. Identification of crack location and magnitude in a cantilever beam from the vibration modes.
12. T. C. TSAI and Y. Z. WANG 1996 *Journal of Sound and Vibration* **192**, 607–620. Vibration analysis and diagnosis of a cracked shaft.
13. R. COLLINS, R. H. PLAUT and J. WAUER 1991 *Transactions of the American Society of Mechanical Engineers Journal of Vibration and Acoustics* **113**, 74–78. Detection of cracks in rotating timoshenko shafts using axial impulses.
14. D. ARMON, Y. BEN-HAM and S. BRAUN 1994 *Mechanical System and Signal Processing* **8**, 81–91. Crack detection in beams by rank-ordering of eigenfrequency shifts.
15. D. SÖFFKER, J. BAJKOWSKI and P. C. MÜKKER 1993 *Transactions of the American Society of Mechanical Engineers Journal of Dynamic Systems, Measurement, and Control* **115**, 518–524. Detection of cracks in turborotors—a new observer based method.
16. S. SEIBOLD and K. WEINERT 1996 *Journal of Sound and Vibration* **195**, 57–73. A time domain method for the localization of cracks in rotors.
17. R. GASCH 1976 *Vibration in Rotating Machinery, ImechE* C178/76, 123–128. Dynamic behaviour of the simple rotor with a cross-sectional crack.
18. R. GASCH 1993 *Journal of Sound and Vibration* **160**, 313–332. A survey of the dynamic behavior of a simple rotating shaft with a transverse crack.
19. R. GASCH 1988 *Vibration in Rotating Machinery, IMechE* C314/88, 463–472. Dynamic behaviour of the Laval rotor with a cracked hollow shaft—a comparison of crack models.
20. A. S. SEKHAR and B. S. PRABHU 1998 *Mechanism and Machine Theory* **33**, 1167–1175. Condition monitoring of cracked rotors through transient response.
21. W. J. GOODWIN 1989 *Dynamics of Rotor–bearing System*. London: Academic of Division of Unwin Hyman Ltd.